

Extension of the Age-of-Fluid Method to Unsteady and Closed-Flow Systems

T. Jongen

Unilever Research, 3133 AT Vlaardingen, The Netherlands

DOI 10.1002/aic.10193

Published online in Wiley InterScience (www.interscience.wiley.com).

The age-of-fluid method is revisited to evaluate and extend it from its traditional application domain of steady, open-flow systems to general unsteady and/or closed-flow systems. The most significant change in the approach comes from the definition of the age of the fluid in a purely kinematic way as a tagging variable, and based solely on the velocity field of the underlying fluid, whereas all the other methods proposed to date somehow determine the age indirectly by tracking an injected tracer material in the flow domain. The resulting mathematical formulation makes it possible to specify the age at arbitrary positions within the flow domain, while being formally very similar to the classical age-of-fluid transport equations previously obtained. This has the benefit of clarifying a number of issues such as the treatment of the diffusion coefficient, the definition of suitable boundary conditions, the validation in unsteady flow conditions, and the extension to closed-flow domains. © 2004 American Institute of Chemical Engineers AIChE J, 50: 2020–2037, 2004

Keywords: age-of-fluid method, closed-flow system, residence time distribution function, flow domain, computational fluid dynamics

Introduction

“Age” is an assessment timescale used in natural and artificial systems as diverse as the ocean and the stratosphere, ground water, processing equipment, migration of biological populations, buildings, and so forth. In biology and chemical reaction engineering it is a well-established technique to represent flows by measuring how long the fluid stays, for example, in a section of the human circulation system (Weinstein and Dudukovic, 1975) or a distillation column (Levenspiel, 1999), and the degree of mixing within a reactor is traditionally assessed by a residence time distribution function, where the residence time is defined as the age of a fluid particle as it leaves the system under consideration. The determination of residence time distributions is of major interest in the design and characterization of most physicochemical and biochemical processes in chemical and biological engineering, where a

proper and homogeneous fluid distribution is often essential (Baléo and Le Cloirec, 2000).

The residence time theory has been generalized and popularized by the pioneering work of Danckwerts (1953) and Zwietering (1959) during the 1950s. Since then, the theory has been refined and extended until it has become one of the most important tools not only in chemical reaction engineering (Levenspiel, 1999; Wen and Fan, 1975), but also in environmental (Sandberg, 1981; Sandberg and Sjöberg, 1983), geophysical (Deleersnijder et al., 2001; Delhez et al., 1999), food and processing (Baléo and Le Cloirec, 2000), biological (Weinstein and Dudukovic, 1975), or pharmaceutical engineering applications (Nauman, 1981). This characterization of flow patterns in terms of age or residence time permits a unified and elegant treatment of open-flow systems (also called continuous-flow systems), which is independent of specific mixing mechanisms. Some flows are so complex that it may prove difficult to gain a profound insight into their functioning by means of a simple inspection of the available values of the basic flow variables. This is why specific interpretation techniques are often needed, some of which demand that an auxiliary variable be estimated.

Current address: Techspace Aero, Route de Liers 121, 4041 Milmort, Belgium; E-mail: tjongen@techspace-aero-be.

Age is one such auxiliary variable. Perhaps not surprisingly, given the widely varying contexts, definitions of age vary. In the present work, and following Delhez et al. (1999), we define the age of a fluid element as the time elapsed since the element under consideration has left the region where its age is prescribed to be zero (which can be on a boundary of the domain of interest, or within the domain). It is also appropriate to conceive the present definition of age as a pointwise, time-dependent variable, an option more general than that adopted in many studies in which the age was defined to be a steady-state quantity (Baléo and Le Cloirec, 2000; Davidson and Olsson, 1987; Spalding, 1958), frequently integrated over a significant fraction of the domain of interest or along its boundaries (Sandberg, 1981).

Age is a concept intimately associated with that of fluid parcels. Hence, evaluating the age in a Lagrangian model is presumably trivial, given that the variables of such a model are “tied” to fluid parcels, rather than being functions of the position in the domain of interest, as must be the case in the Eulerian description of fluid flows. On the other hand, most of the transport phenomena models are formulated in a Eulerian way. Therefore, for a given Eulerian model, it is tempting to recommend that a Lagrangian module be included at least for the purpose of computing the age. This is the route that a number of current computational fluid dynamics (CFD) packages have taken. Nonetheless, this may not be the best option, for several reasons. First, Lagrangian solvers, such as that described in Hunter et al. (1993), demand generally more computer time than their Eulerian counterparts. Second, the age, as a diagnostic quantity or prognostic model parameter, should be evaluated by means of an algorithm as similar as possible to the one used in the computation of the other transported variables, which is here assumed to be Eulerian. Third, it would be necessary to inject and track a large quantity of Lagrangian fluid parcels to obtain a suitable density of particle paths to generate spatial distribution maps, which are easier to obtain from Eulerian results. This would become even worse in the case of unsteady flows where this procedure would have to be repeated over many small time intervals.

In the present study, a strictly kinematic definition of age is used. The age is seen as a purely passive and advected scalar diagnostic variable and is not derived from conservation principles as is the case in the classical theory of age. The advantage of such a formulation is that age can then be set to an arbitrary value anywhere in the flow domain, as will be seen later. This kinematic definition of age implies that the diffusive and nonresolved subgrid mixing processes are neglected, which means that all the transport scales are supposed to be explicitly resolved by the model and any transport of matter proceeding at velocity $\mathbf{u}(t, \mathbf{x})$ is viewed as advection. The age is therefore a property of the underlying fluid only, where no diffusion or subgrid transport processes have to be accounted for and superimposed to the resolved, bulk convection from the flow field. The age defined in such a way will be called “advective age,” and can be seen as the Eulerian transposition of the Lagrangian age, for which there is no such thing as diffusion or subgrid mixing along a particle path. This is in contrast to many previous studies (Baléo and Le Cloirec, 2000; Davidson and Olsson, 1987; Delhez et al., 1999; Sandberg and Sjöberg, 1983; Spalding, 1958) where age was a physical property derived from the conservation laws of an injected

tracer constituent. As will be shown herein, the classical “material age” formulation leads to a number of limitations and issues in the methodology for the case where one is interested in the age of the underlying fluid and not in the transported species itself. In particular, one of the main limitations is certainly the impossibility of using the material age formulation in a closed-flow system, such as a recirculation region or a batch system because age becomes infinite in such regions. Another problem is the need to specify a diffusion coefficient as a consequence of the fact that the age is derived from an injected physical tracer. Also, it is impossible to reset the value of the age to a specified value at arbitrary positions within the flow domain because it would violate mass conservation.

Figure 1 gives a two-dimensional (2-D) illustration of the various situations that will be addressed in the present work. Figure 1a shows the regions (labeled \mathbf{R}_1 , \mathbf{R}_2 , and \mathbf{R}_3) where the age [noted $a(t)$] is set to a fixed reference value (0 in the present case). Regions \mathbf{R}_1 and \mathbf{R}_2 correspond to the inlet sections of the flow domain, where imposing an age equal to zero poses no difficulties. The principal objective of this paper is to present a method to reset the age at arbitrary positions within the domain, such as along the zone \mathbf{R}_3 in the figure. Its use can be appreciated by considering the evolution of age along several fluid paths, as illustrated in Figure 1b. Streamlines s_1 , s_2 , and s_3 correspond to the case of an open-flow system, with s_3 having its age reset within the domain as it crosses the zone \mathbf{R}_3 . Streamlines s_4 and s_5 correspond to a closed-flow system situation, where s_4 maintains a bounded age because it also crosses the reset zone \mathbf{R}_3 , but s_5 has an unbounded age, which increases at the same rate as the simulation time.

Two standard age-of-fluid formulations are first reviewed in the following section, and their limitations highlighted. The proposed formulation for the advective age is then derived from a purely Lagrangian perspective and extended to unsteady and closed-flow systems. Specific comments on the numerical implementation of the resulting advective age evolution equation and suitable boundary conditions are given at the end of that section. Examples illustrating the potential of the extended formulation are then presented to validate the new methodology.

Equations for the Age of Fluid

The basic relations governing the evolution of the fluid age are derived in this section. This gives the motivation for an extension of the age-determination methodology, which is derived afterward together with a discussion on boundary conditions and numerical implementation.

Standard age-determination method

The traditional way to determine the spatial distribution of age in a computational framework (Spalding, 1958) derives from the experimental approach used in chemical engineering (Danckwerts, 1953; Levenspiel, 1980). Age can be measured experimentally at any point of an open-flow domain (also called continuous flow) by injecting a pulse of tracer material into the inlet at a given reference time (say $t = 0$) and by recording continuously the concentration $C(t, \mathbf{x})$ of the tracer at the point \mathbf{x} under consideration. From its distribution function Φ_C , defined as

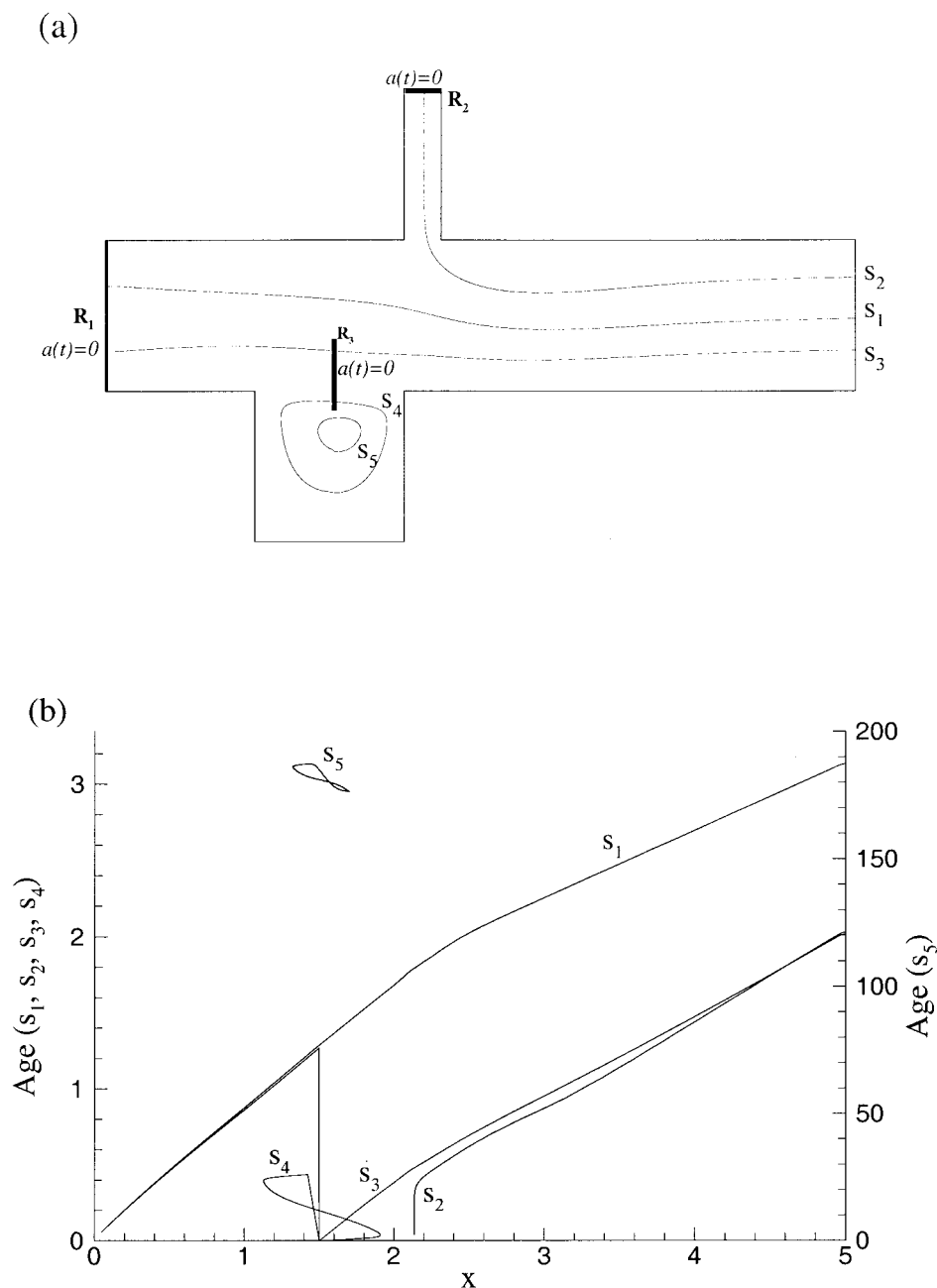


Figure 1. Two-dimensional illustration of the various situations addressed in the present work.

(a) The regions labeled R_1 , R_2 , and R_3 correspond to zones where the age is reset to 0. Fluid paths s_1 , s_2 , and s_3 correspond to the case of an open-flow system, with s_3 having its age set to 0 within the fluid domain. Particle paths s_4 and s_5 correspond to a closed-flow system situation. (b) Evolution of the age along the fluid paths s_1 to s_5 as a function of the horizontal coordinate x .

$$\Phi_C(t, \mathbf{x}) = \frac{C(t, \mathbf{x})}{\int_0^\infty C(s, \mathbf{x}) ds} \quad (1)$$

it is possible to determine the local age a as its first moment,

$$a(\mathbf{x}) = \int_0^\infty t \Phi_C(t, \mathbf{x}) dt \quad (2)$$

It should be noted that this definition of age leads to a quantity that is independent of time and is therefore applicable only in a steady-state context. This limitation is essentially linked to the experimental procedure, which is based on recording and integrating a time-dependent tracer signal and assumes that the underlying transport field does not vary in time.

To obtain an equation for the age in a computational context, the standard scalar advection–diffusion equation governing the evolution of the concentration of the tracer material is multiplied by t and integrated from 0 to ∞

[assuming $C(0, \mathbf{x}) = C(\infty, \mathbf{x}) = 0$, which is the case for a pulse]

$$-\int_0^\infty C dt + \mathbf{u} \cdot \nabla \int_0^\infty C dt = \nabla \cdot \left(K_C \nabla \int_0^\infty C dt \right) \quad (3)$$

where, as noted previously, the velocity field \mathbf{u} is assumed to be steady (and incompressible) and K_C is the diffusion coefficient of the tracer material used for the experiment. Because the left-hand side of Eq. 3 is constant (a finite amount of tracer material has been injected during the pulse), the whole equation can be divided by the lefthand side, as follows

$$\nabla \cdot (\mathbf{u}a - K_C \nabla a) = 1 \quad (4)$$

which is the classical transport equation giving the spatial distribution of age for the tracer material. Most computational methods for the evaluation of the age in chemical engineering or HVAC use this equation (Sandberg, 1981; Spalding, 1958). However, this method suffers from two main limitations, both a consequence of its inspiration from the experimental procedure. First, Eq. 4 is applicable to steady flows only. This is attributed to the definition of age (Eq. 2) based on the tracer signal. Second, the method is intrinsically linked to a passive tracer, and can therefore measure the age of the passive tracer only, and not the kinematic age of the underlying fluid, which is not subjected to the same diffusion mechanisms as the tracer material. A diffusion coefficient K_C has to be included, which makes sense in an experimental context where a tracer material is actually used. In a computational context, however, there is little use or guidance as to the value of this diffusion coefficient. The use of a nonzero diffusion for the computation of the age of the underlying fluid distorts the results and moves its use away from a purely diagnostic tool. Of course, this limitation does not hold if one is looking for the age of the passive tracer itself, such as in studies of pollutant dispersal.

General theory of age

In recent years a general theory of age has been developed (Deleersnijder et al., 2001; Delhez et al., 1999) from population balance modeling considerations. This theory is applicable to multicomponent and unsteady systems, and takes into account advection, diffusion, production, and destruction processes of scalar tracers. It also distinguishes between the age of a particular species in a fluid mixture, of an aggregate of species, and of the total mixture, with the age of every constituent depending on time and position. In addition, it is suited for problems in which there is either a species source located on the boundaries of the domain of interest (such as an inlet) or within the domain of interest (such as a source region for time-dependent problems). Moreover, the species source can be pointwise or distributed over a region. This theory provides a first coherent and rigorous framework from which most of the forms previously suggested in the literature may be derived after certain simplifications and hypotheses.

For the present purpose of computing the advective age (that is, the age of the underlying fluid), the particular case of flow systems consisting of only one component (the fluid itself) will

be used. The detailed developments pertaining to the general theory of age, including the case of age of individual species, can be found in Deleersnijder et al. (2001) and Delhez et al. (1999). At the core of the theory is the age distribution function $c(t, \mathbf{x}, \theta)$, defined as the fraction of material present at time t at position \mathbf{x} , whose age is equal to θ . In this definition the age θ is an independent variable, which must not be mistaken for the mean age a , a dependent variable defined as

$$a(t, \mathbf{x}) = \int_0^\infty \theta c(t, \mathbf{x}, \theta) d\theta \quad (5)$$

Using population-balance theory considerations, it can be shown (Deleersnijder et al., 2001) that the age distribution function $c(t, \mathbf{x}, \theta)$ satisfies a generalized advection–diffusion equation where phenomena such as production and destruction of age, and transport processes that are resolved (advection) and nonresolved (subgrid mixing), are accounted for rigorously. The final form that is obtained in the case of a single species (the fluid itself) in terms of the age of fluid, is given by

$$\frac{\partial}{\partial t} a + \nabla \cdot (\mathbf{u}a - \mathbf{K} \cdot \nabla a) = 1 + \mathcal{P} - \mathcal{D} \quad (6)$$

with

$$\mathcal{P}(t, \mathbf{x}) = \int_0^\infty \theta p(t, \mathbf{x}, \theta) d\theta \quad \text{and} \quad \mathcal{D}(t, \mathbf{x}) = \int_0^\infty \theta d(t, \mathbf{x}, \theta) d\theta \quad (7)$$

where p (≤ 0) and d (≤ 0) are the rate of age production and destruction, respectively (that is, the source and sink terms of material of age θ), and \mathbf{K} is a diffusivity tensor accounting for the advection phenomena that are not explicitly resolved by the model. This is the rigorous generalization of the age Eq. 4 obtained in the previous section. It can cope with unsteady-flow situations, and accounts for mixing and diffusion processes in a correct manner. The key aspect of the theory is that the mean age equation is derived from the age distribution function and therefore can rigorously account for production, destruction, and subgrid mixing processes. This theory is very powerful in the cases where one is interested in the age distribution of various species in a multicomponent flow.

Another useful feature of the theory is the possibility to inject a species within the flow domain (and not only on its inlet boundaries as in the standard method) and follow the evolution of its age as it is transported away from its source. A similar feature will be used later when the concept of age is extended from open-flow systems to closed-flow systems. In this case, it will be necessary to “reset” the age of fluid elements to a reference value (such as zero) as they pass over a prescribed region within the flow domain. In the general theory of age, this would be achieved by injecting a species in the flow through the “reset” region, given that the newly

injected material will have an age equal to zero by definition. This would pose no particular problem (Deleersnijder et al., 2001) and could be achieved through the correct choice of the age production and destruction terms \mathcal{P} and \mathcal{D} in Eq. 6. However, in the present case of a single fluid (or the whole fluid mixture), it is not possible to inject additional fluid material without violating mass conservation or without defining the point of injection as a new boundary of the domain. In a computational context, the latter solution of creating a new boundary to the computational domain is obviously not convenient and will not be considered. The problem generated by the former solution is also problematic because the age distribution function has to account for the totality of the fluid material at time t and location \mathbf{x}

$$\int_0^\infty c(t, \mathbf{x}, \theta) d\theta = 1 \quad (8)$$

From this, a constraint on the age production and destruction terms is obtained

$$\int_0^\infty p(t, \mathbf{x}, \theta) d\theta = \int_0^\infty d(t, \mathbf{x}, \theta) d\theta \quad (9)$$

which means that in the case of a single fluid (or the whole fluid mixture), it is not possible to impose a source of zero age inside the flow domain because setting $\mathcal{P} \neq 0$ in Eq. 6 would be cancelled out by a destruction term such that $\mathcal{D} = \mathcal{P}$.

In conclusion, it appears that the general theory of age is a powerful framework for unsteady and multispecies flow systems, but for the present purposes of the computation of the advective age of the underlying fluid, the theory does not provide the freedom to design the age source term appropriately over “reset” regions. The general age theory is therefore inadequate, and a different formulation is required. The main reason for this inadequacy is that age is derived from tracking a physical tracer material, which has to follow the mass conservation rules and cannot serve as a purely kinematic “tagging” variable.

Equation for the advective age

The age-computation methods highlighted above are representative of virtually all the approaches for the determination of the age of a fluid. In addition to the limitations reviewed in the previous sections, two additional problems have to be mentioned. First, these methods have been developed for open-flow systems, probably because it seems to make little sense to inject a tracer material in a closed-flow region. The proper handling of recirculation zones (“dead” volumes where the advective age is—paradoxically—infinite) is still lacking, although valuable information on the flow along closed streamlines could be gained through a different approach, as will be shown shortly. Second, an appropriate treatment of the boundary conditions for solid (or more generally nonpenetrating) boundaries has not yet been proposed. From a tracer material perspective, there is no transport of tracer through a solid boundary, and the classical recommendation is therefore to

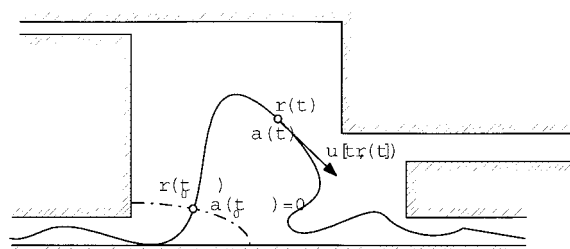


Figure 2. A fluid particle path with the position, velocity, and age vectors.

impose a zero-flux condition ($\partial a / \partial n = 0$) on the boundary, with n the normal direction. This, however, is in conflict with the fact that the advective age and its normal derivative are theoretically infinite on solid boundaries.

To meet the requirements of an advective age tracer applicable to steady- or unsteady-, open- or closed-flow systems, and whose value can be reset to zero inside portions of the flow domain, it is necessary to start from the basic signification of the age of a fluid parcel, which is intimately linked to a Lagrangian description. The age of a fluid element is defined as the time elapsed since the element under consideration left the region in which its age is prescribed to be zero, which may be zero- to 3-D (that is, a point, a curve, a surface, or a volume). The nature of the region where the age is prescribed to be zero obviously depends on the flow system considered and the purpose for which the age is introduced. Consider a fluid parcel following a path described by its position vector $\mathbf{r}(t)$ at time t (Figure 2). By definition of a trajectory, $\mathbf{r}(t)$ is related to the fluid velocity between two instant t_0 and t by the expression

$$\mathbf{r}(t) = \mathbf{r}(t_0) + \int_{t_0}^t \mathbf{u}[s, \mathbf{r}(s)] ds \quad (10)$$

It follows that the age $a[t, \mathbf{r}(t)]$ of the fluid parcel present at position \mathbf{r} at time t is simply given by

$$a[t, \mathbf{r}(t)] = t - t_0 + a[t_0, \mathbf{r}(t_0)] \quad (11)$$

In line with the definition of age, we can assume that t_0 is the time when the fluid parcel under consideration has left the region where the age is zero: $a[t_0, \mathbf{r}(t_0)] = 0$. Using those relations, the fundamental expression is obtained

$$\mathbf{r}(t) - \mathbf{r}(t_0) = \int_{t-a[t, \mathbf{r}(t)]}^t \mathbf{u}[s, \mathbf{r}(s)] ds \quad (12)$$

which simply says that the advective age of a fluid parcel is the time elapsed along its path. Although Eqs. 11 and 12 are the closest to the definition of the advective age of a fluid element, their implicit and Lagrangian form makes them of limited practical use in a Eulerian computational context. A useful transport equation for the age of fluid is easily obtained by taking the derivative of Eq. 11 along the fluid parcel's path

$$\frac{D}{Dt} a[t, \mathbf{r}(t)] = 1 \quad (13)$$

or its Eulerian equivalent,

$$\frac{\partial}{\partial t} a + \nabla \cdot (\mathbf{u}a) = 1 \quad (14)$$

Although formally equivalent to Eq. 6 without diffusion ($\mathbf{K} = 0$) and source or destruction terms ($\mathcal{P} = \mathcal{D} = 0$), which was derived from the general theory for the material age, the present concept of age has a fundamental difference in the fact that it is not derived from an underlying tracer material advection–diffusion consideration. It is now possible to set in Eq. 14 the value of the age to any prescribed value within the domain of interest, and not only at the boundaries of the domain. For this, \mathbf{R} is defined as the region where the age is set to a reference value a_R (typically $a_R = 0$). Obviously, \mathbf{R} is a subset of the flow domain, and can be a zero- to 3-D domain.

Although this framework allows the age distribution to be arbitrarily modified within the domain without violating any conservation principle, the appropriate formulation of such a requirement is not trivial in the context of differential equations. Initial and boundary-value problems usually do not allow the solution to be directly specified within the domain. A well-known (Patankar, 1980) way to impose a value a_R on an internal region \mathbf{R} is to define a zero-age distribution function f_R such that

$$f_R(\mathbf{x}) = \begin{cases} 1 & \text{for } \mathbf{x} \in \mathbf{R} \\ 0 & \text{otherwise} \end{cases} \quad (15)$$

The required behavior of the age is then obtained from a suitable definition of the source term in Eq. 14

$$\frac{\partial}{\partial t} a + \nabla \cdot (\mathbf{u}a) = 1 - f_R[1 - c(a_R - a)] \quad (16)$$

where $c > 0$ is a relaxation parameter. The solution obtained is approximate in the sense that in the case of a steady computation, this formulation will give the correct solution of Eq. 14 outside the reset domain \mathbf{R} and give the value a_R over \mathbf{R} , as expected, except over a thin transition layer around the edges of \mathbf{R} . In a transient context, an extra relaxation effect will also have to be taken into account.

Equation 16 is the final form of the advective age transport equation that is solely based on kinematic considerations and is applicable to both open- and closed-flow systems, and to unsteady systems. It gives the possibility to “reset” the age function directly in the flow domain, a useful feature in the case of closed-flow systems, as will be seen later. Note also that there is no diffusion coefficient to define.

As mentioned above, Eq. 16 is a simple and robust way to match the solution to a specified value over a portion of the domain. As a streamline enters the “reset” domain \mathbf{R} , the value of age will be driven to the reference value a_R at a certain rate, dependent on the value of the parameter c and the local velocity

magnitude u_R . Because by definition $f_R = 1$ over the region \mathbf{R} , the steady age Eq. 16 simplifies to the relaxation equation

$$\nabla \cdot (\mathbf{u}a) = c(a_R - a) \quad (17)$$

Using $a_R = 0$ and assuming that the characteristic velocity on the streamline over the region \mathbf{R} is equal to u_R , this reduces to

$$u_R \frac{\partial a}{\partial x} = -ca \quad (18)$$

or

$$a(x) = a(0)e^{-cx/u_R} \quad (19)$$

Representing the typical streamwise “thickness” of \mathbf{R} by ΔR , the previous equation can then be used to set the coefficient c as a function of ΔR and the desired age reduction factor $\varepsilon = a(\Delta R)/a(0)$

$$c \sim -\frac{u_R}{\Delta R} \ln(\varepsilon) \quad (20)$$

This relation can be used as a lower bound to set the value of c as a local or global parameter. From a purely numerical standpoint, the reset region will impose a requirement on the spatial and temporal resolution, so that the age is numerically able to relax as it passes through \mathbf{R} . In practice, a balance will have to be found between the speed of reduction of the age within \mathbf{R} and the resulting stiffness of the iterative solution scheme.

Boundary conditions and numerical considerations

Given a steady or unsteady velocity field \mathbf{u} and a zero-age domain distribution function f_R , the advective age can be obtained by solving the scalar advection equation with source-term (Eq. 16). Given that virtually all the numerical discretization and algorithms that have been developed and implemented in computer codes are adapted for scalar advection–diffusion equations, the age transport Eq. 16 can easily be solved in the same framework. The special form of the source term, with potential discontinuities through the zero-age function f_R , should not lead to particular problems, and convergence could be tuned through the stiffness parameter c discussed in the previous section. Similarly, no specific loss of accuracy should be expected because the age distribution obtained as a solution of Eq. 16 will still be a smooth function, even if the source term has discontinuities. Difficulties may arise, however, because of the purely advective character of the age transport equation. Artificial diffusion effects of the discrete solution will be unavoidable because of numerical diffusion (Patankar, 1980). Classical advection–diffusion discretization schemes also require boundary conditions on all domain boundaries, whereas the age transport equation, strictly speaking, provides conditions only at the domain inlets, and even has a singular behavior on solid boundaries and in (steady) recirculation zones, where the age is theoretically infinite.

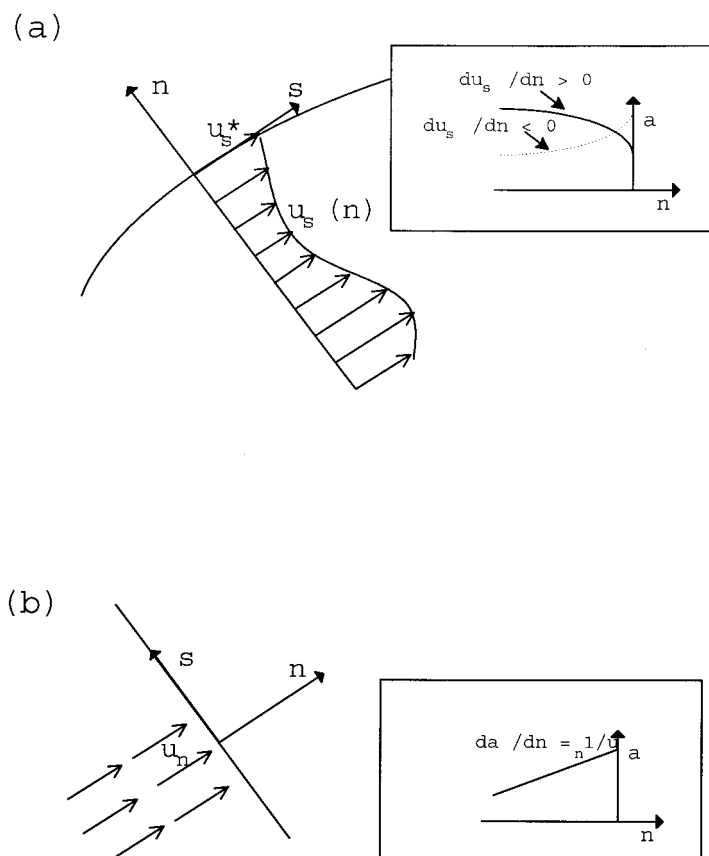


Figure 3. (a) Reference system for a slip or shear boundary. (b) Reference system for an outlet boundary.

The case of infinite values will be addressed first. For this, the following transformation of variables is defined

$$v \equiv \frac{1}{\alpha a + \beta} \quad (21)$$

where α and β are constants. Injecting this expression into the transport Eq. 16 for the age a , an equivalent transport equation for v can be derived

$$\frac{\partial}{\partial t} v + \nabla \cdot (\mathbf{u} v) = -\alpha v^2 + f_R \left[\alpha v^2 + \frac{c}{\beta} (v_R - v) \right] \quad (22)$$

where $v_R = (\alpha a_R + \beta)^{-1}$. The solution of Eq. 22 with Eq. 21 is theoretically equivalent to the solution of Eq. 16. In terms of their discrete numerical equivalent, however, Eq. 22 has the computational advantage of dealing with infinitesimal values instead of infinite values because $v \rightarrow 0$ as $a \rightarrow \infty$. The choice of the coefficients $\alpha \neq 0$ and β is arbitrary and should provide the appropriate scaling to facilitate the computations. For instance, the inlet condition $a = 0$ implies that $v = 1/\beta$, which means that β should be chosen such that $\beta \neq 0$. Similarly, a choice $\alpha > 0$ and $\beta > 0$ guarantees that $0 \leq v \leq 1/\beta$ and makes the source term in Eq. 22 negative, which greatly helps the computational stability. A small (positive) value of α would also help smoothing out the spatial gradients, given that Eq. 21 leads to

$$\frac{\partial}{\partial x_j} v = -\alpha v^2 \frac{\partial}{\partial x_j} a \quad (23)$$

Loosely speaking, the transformation Eq. 21 helps to transfer some of the stiffness of the differential equation to an algebraic stiffness through the appropriate scaling parameters α and β . Note that the new variable v can be interpreted as a generalized “ventilation rate” and is often used in the field of building engineering as a measure of the exchange of “fresh” material at a point (Sandberg and Sjöberg, 1983).

Concerning the appropriate definition of boundary conditions, it is important to realize that the purely convective character of transport equations such as Eq. 16 or, equivalently, Eq. 22 require in theory the definition of boundary conditions only on ingoing characteristics (that is, along the inlet boundaries of the flow system). In practice, however, such equations are solved using existing advection–diffusion equation solvers, which require conditions on all boundaries. The ambiguous character of these additional boundary conditions has left questions about their proper treatment. The important cases of slip, nonslip, and outlet boundary conditions are discussed hereafter.

Consider first the case of slip boundaries, such as a free stream or a moving wall, or stress boundaries, as shown in Figure 3a. The corresponding boundary conditions on the momentum equations are $\mathbf{u} \cdot \mathbf{s} \equiv u_s = u_s^*$ and $\mathbf{u} \cdot \mathbf{n} \equiv u_n = 0$, or $\partial u_s / \partial n = \gamma^*$, where \mathbf{s} and \mathbf{n} are the local tangent and normal

vectors to the boundary, and u_s^* and γ^* are the imposed slip or shear rate values. Very close to the boundary, the velocity will be essentially parallel to the boundary, and in the local reference system (\mathbf{s} , \mathbf{n}), assuming steady flow conditions, the age equation simplifies to

$$u_s \frac{\partial}{\partial s} a = 1 \quad (24)$$

It is also assumed that close enough to the boundary the tangential velocity component u_s is a function of the normal coordinate n only. This is obviously true when the slip velocity is a constant, and should hold in most other cases. The solution of Eq. 24 close to the boundary is

$$a(s, n) = \frac{s}{u_s(n)} + a_0(n) \quad (25)$$

where $a_0(n)$ is the age profile along the reference coordinate $s = 0$, which can be taken as $a_0 = 0$ without loss of generality. Deriving this expression with respect to the normal coordinate

$$\frac{\partial}{\partial n} a = -\frac{s}{u_s^2} \frac{\partial}{\partial n} u_s = -\frac{a}{u_s} \frac{\partial}{\partial n} u_s \quad (26)$$

Equation 26 is the improved boundary condition to apply at prescribed slip or shear boundaries. It also shows that the default homogeneous boundary condition $\partial a / \partial n = 0$ that is usually applied is valid only in the case where $\partial u_s / \partial n = 0$, such as along a symmetry line. In terms of the new variable v defined in Eq. 21, the boundary condition (Eq. 26) for slip or shear boundaries is expressed as

$$\frac{\partial}{\partial n} v = \frac{v}{u_s} \frac{\partial}{\partial n} u_s (1 - \beta v) \quad (27)$$

The case of nonslip boundaries, such as solid walls, also requires special attention. Given that, in this case, the velocity u_s vanishes, the boundary condition (Eq. 26) is not useful because the age is infinite on a solid boundary, as well as its normal derivative. In terms of the new variable v , however, the correct boundary condition is remarkably simple

$$v = 0 \quad (28)$$

Here also, the traditional approach has been to impose a zero-gradient condition $\partial a / \partial n = 0$ at the wall, obviously a wrong condition for a purely kinematic age tracer.

Finally, the case of outlet boundary conditions needs to be addressed. As for the other boundaries, most previous works use the condition $\partial a / \partial n = 0$ with the notations used in Figure 3b. This is incorrect because the age increases along outgoing particle paths. On the other hand, it can be expected that the upstream influence of this boundary will be limited because of the (theoretically) purely advective character of the age equation. A simple improvement of this boundary condition, however, can be obtained as follows. Using the standard outflow

condition of fully developed flow $\partial u_n / \partial n = 0$, the solution of the age Eq. 16 along an outgoing particle path is

$$a(s, n) = a_0(s) + \frac{n}{u_n} \quad (29)$$

with a_0 a reference value. This leads to the improved outflow boundary condition

$$\frac{\partial}{\partial n} a = \frac{1}{u_n} \quad (30)$$

or, in terms of the variable v

$$\frac{\partial}{\partial n} v = -\frac{\alpha v^2}{u_n} \quad (31)$$

Illustrations

Applications of these considerations to different cases are presented below. Starting with the basic situation of a steady open-flow system, extensions to unsteady and to closed-flow systems are presented using a number of illustrative cases with an increasing degree of complexity.

Steady open-flow system

Validation of the classical age-of-fluid evolution Eq. 4 is performed by considering a typical open-flow system (Figure 4). The setup has been chosen such that the steady-flow field is sufficiently complex to provide a realistic illustration, and has a few interesting features such as two inlet regions (that is, two different age sources) and a closed recirculation in the cavity. The steady distribution of the fluid age has been computed from Eq. 22 with $\alpha = \beta = 1$ and with no age-resetting sources in the domain ($f_R = 0$).

The fluid and age transport equations have been solved using the commercial computational fluid dynamics (CFD) software CFX5.1 provided by AEA Technology (CFX-5.1 User Manual, 2003). The numerical solution to the flow and transport equations is obtained using a first-order finite-volume discretization based on an unstructured mesh. The mesh density used ($>10,000$ nodes) is sufficiently high to guarantee a grid independence of both flow and age solutions.

The resulting contour lines of the ventilation rate v are shown in Figure 5a, and the corresponding distribution of the fluid age derived from Eq. 21 is shown in Figure 5b. As expected, values of the ventilation rate v decrease rapidly from their inlet value 1, and the relatively “younger” contribution from the fluid coming from the vertical inlet can be easily identified. Values of the ventilation rate are very close to 0 in the recirculation zone, as well as in the vicinity of the solid walls. In terms of fluid age, this means that very high values are attained in those regions, and should theoretically become infinite. In practice, the simulations are usually evolved from an initial state through a transient phase until convergence is considered to be achieved. In the case of the age Eq. 16, even if the underlying flow field has reached a steady state, the values of age will continue to increase indefinitely in the recirculation zone (that is, along closed streamlines), at the

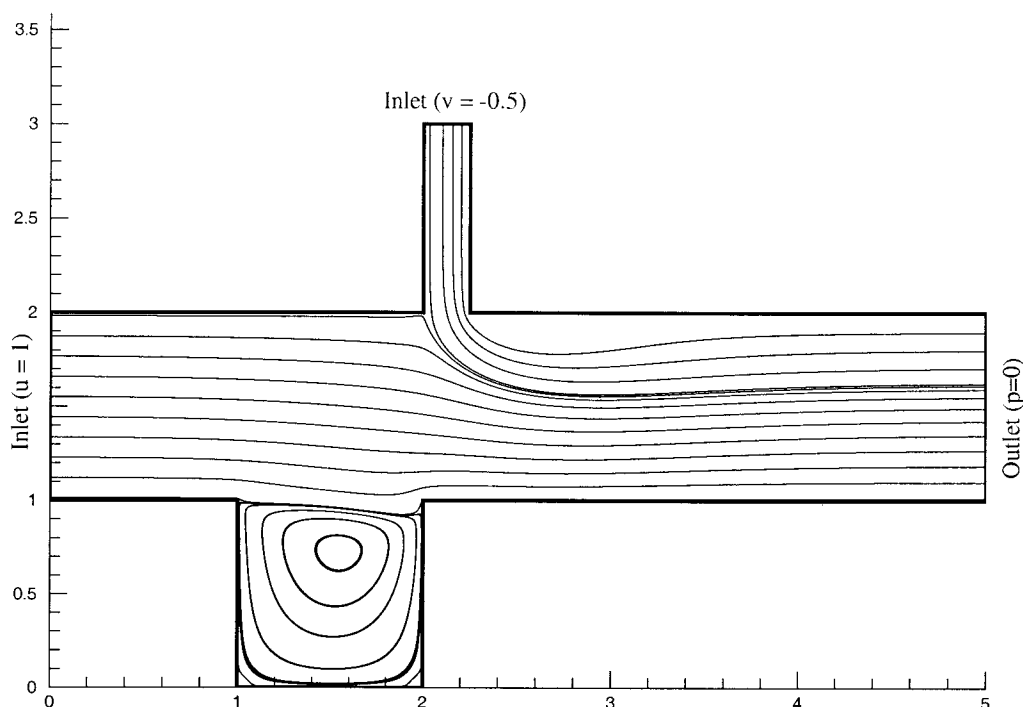


Figure 4. Streamlines of the 2-D, steady-flow validation case.

same rate as the simulation time increases. For instance, the value of the age at the center of the recirculation zone in Figure 5b is approximately 80, which corresponds roughly to the physical time during which the transient solution has been propelled toward a steady state, as will be explained in a subsequent section. There are two reasons why all the points contained within the recirculation zone (that is, below the dividing streamline) do not have exactly the same age. The first reason is that during the initial velocity transient, some “fresh” fluid has been mixed with the fluid initially contained in the cavity. It is only when the velocity field is established that all the fluid parcels within the recirculation zone are ageing at the same rate. This would not be the case if the age equation was solved on an already established flow field. Second, some degree of numerical diffusion between the open-flow and the closed-flow domains cannot be avoided. As the age in the recirculation region continues to increase, the gradient of age across the dividing streamline will become so large that significant diffusion will eventually take place across the open and the closed regions, until an equilibrium is reached between the diffusive flux generated by the numerical discretization and the rate of ageing in the cavity. The same reasoning applies to near-wall regions where truly infinite values will not be achieved, irrespective of the numerical accuracy of the advective scheme used in the simulation.

The real acid test for the method comes from comparing the age computed by its evolution Eq. 16 or Eq. 22 to the “real” Lagrangian age obtained by integrating the residence time along injected particle paths (Eq. 10)

$$t - t_0 = \int_{r_0}^r \frac{1}{\|\mathbf{u}\|} d\mathbf{r} \quad (32)$$

This test is a very challenging test for the method because it really compares the Eulerian representation of age to its Lagrangian equivalent after discretization. This kind of systematic test is seldom performed, especially using exactly the same numerical solution. To the author’s knowledge, most previous validation works were restricted to comparisons with experimental data obtained on comparable flow configurations (Baléon and Le Cloirec, 2000).

Using the particle paths shown in Figure 5b, Figure 6 compares the age obtained from the two methods. The solid lines correspond to the values of the age field computed from Eq. 16 or Eq. 22 and extracted along the injected particle paths, whereas the dashed lines correspond to the evolution of the age integrated with Eq. 32 along the same particle paths. As can be seen, the two results compare reasonably well, and the discrepancies must be attributed to the numerical diffusion polluting the otherwise purely advective process. Even a particle path very close to the solid boundaries (streamline labeled s_5 in Figure 6) shows a relatively good agreement, although it travels within a region with a very high age gradient. Also, it is interesting to note that along closed paths (labeled s_4 in Figure 6), the age computed from the transport equation has to form a closed curve because the age is a smooth field in the flow domain and must therefore decrease at some point. On the other hand, the Lagrangian age computed following a particle path is always increasing. This apparent contradiction can be explained as follows. As noted above, the intrinsically transient character of the age transport equation over closed-flow regions has to be taken into account. The whole closed curve, shown at a given time in Figure 6, will actually continue to move vertically on the graph as time goes by, at such a rate that the fluid particles following the closed path would still see their age increasing, even through the apparent “dips” on the Eulerian representation.

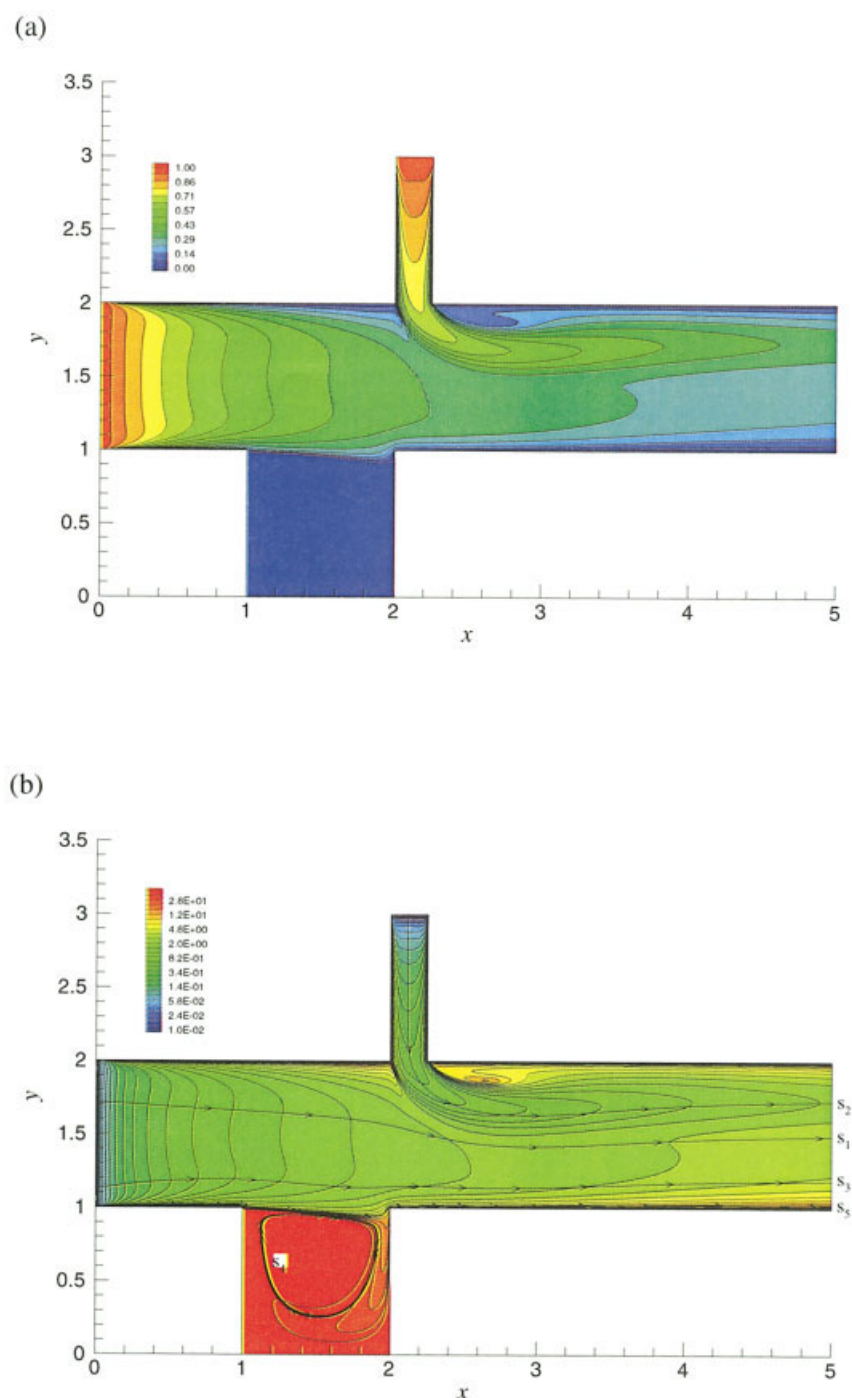


Figure 5. (a) Contour lines of the ventilation rate v . (b) Contour lines of the age a (note the logarithmic scale on the legend).

Simple 1-D unsteady systems

The next level in complexity comes from the extension of the age-of-fluid concept to unsteady flow situations. As explained in the previous section, the age variable $a(x, t)$ at a point x and time t should be interpreted in a broader sense as the time elapsed since the fluid parcel present at time t and at position x has left the region in which its age was prescribed to be zero. Because in this case both the flow and age fields

depend on time, it is necessary to integrate them together, and not in an a posteriori diagnostic manner as was the case for steady flows, where the age could be computed on a previously obtained flowfield. Because the visualization and interpretation of the results are also more difficult, a preliminary study on a simple unsteady 1-D system might offer valuable preliminary insights.

Consider the simple case of a 1-D plug flow moving in the

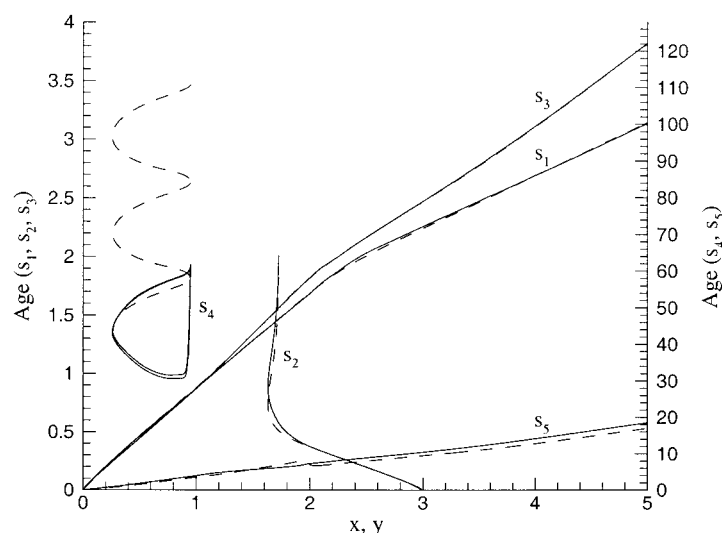


Figure 6. Evolution of the age along the streamlines shown in Figure 5b.

Age computed from the evolution Eq. 22 (—); age computed from its Lagrangian definition (---).

direction x with a time-varying velocity function $u = u(t)$. Note that by incompressibility u must be constant in space (in x) at any time. The age can be defined to be zero at the “inlet” $x = 0$, and the subsequent evolution of the spatiotemporal distribution of age within the domain (x, t) , with $x, t \geq 0$ can be visualized.

Different velocity time-variation patterns can be studied. In the trivial case of a steady velocity $u = u_0$, the age distribution $a(x, t)$ is simply given by

$$a(x, t) = x/u_0 \quad (33)$$

which is obviously independent of time. The next case is a sudden change in the velocity, from $u = u_1$ to $u = u_2$ at time $t = t_1$. To obtain the spatiotemporal age distribution, Eq. 12 turns out in this simple 1-D case to lend itself to an easier manipulation than Eq. 14. For times $t < t_1$, the velocity has not yet changed, and the solution is similar to the steady situation, $a(x, t) = x/u_1$. Similarly, for all times and locations such that $t > t_1 + a = t_1 + x/u_2$, the material elements have passed through the inlet $x = 0$ after the step change in velocity, and will therefore not be affected by it: $a(x, t) = x/u_2$. Finally, for intermediate times

$$x = \int_{t-a}^{t_1} u_1 dt + \int_{t_1}^t u_2 dt = u_1 a + (u_2 - u_1)(t - t_1) \quad (34)$$

from which an expression for the age a can be obtained. Figure 7 shows different representations of the evolution of the age, including contours of constant age in the (x, t) plane (Figure 7b), where the dashed lines correspond to particle paths originating from the initial state at $t = 0$ or injected from the inlet. For fluid elements present in the system during the velocity transition, the effect of history is very clear, and the sudden fluid acceleration is building up into a linear decrease of the age until all the particles that have experienced the velocity transition have been washed out of the system boundaries. This

zone is clearly defined by the dividing particle path originating from the inlet $x = 0$ at time t_1 .

Unsteady open-flow systems

To further illustrate the extension of the age-of-fluid transport Eq. 16 to unsteady situations, a sufficiently complex time-varying flow has to be chosen. A good choice for such a flow is the mixing of two fluids where two streams of differing uniform velocity are brought together at the edge of a two-dimensional splitter plate. Downstream, the two fluids mix, and momentum diffuses across the interface. It can be shown (Hama, 1962) that for large enough Reynolds numbers, the flow downstream has a velocity that to a good approximation is unchanging with x , with velocity components

$$u = 1 + \tanh(y) \quad \text{and} \quad v = 0 \quad (35)$$

Note that in this example, the low-speed stream is actually quiescent. If small disturbances are added to this flow, the flow is destabilized and they cause the vorticity in the layer to roll up into discrete vortices (which will eventually become turbulent). As shown in Hama (1962), the resulting unsteady perturbed base flow can be expressed as

$$\begin{aligned} u(x, y, t) &= 1 + \tanh(y) + 2\zeta \tanh(y) \operatorname{sech}(y) \sin(x - t) \\ v(x, y, t) &= 2\zeta \operatorname{sech}(y) \cos(x - t) \end{aligned} \quad (36)$$

where ζ is a small number, taken here as $\zeta = 0.05$. This unsteady velocity field will be used to compute the time and space distributions of the fluid age from Eq. 16, and compare the age field to the residence times obtained by integrating the Lagrangian age along injected particle paths, as was done previously for the steady validation. Figure 8 shows flow streamlines at time $t = 30$ (solid lines), as well as streaklines obtained by continuously injecting tracer particles at $(x, y) = (0, 0)$. The unsteady character of the flow and the roll-up of vortices are clearly visible. With such a complex flow, the

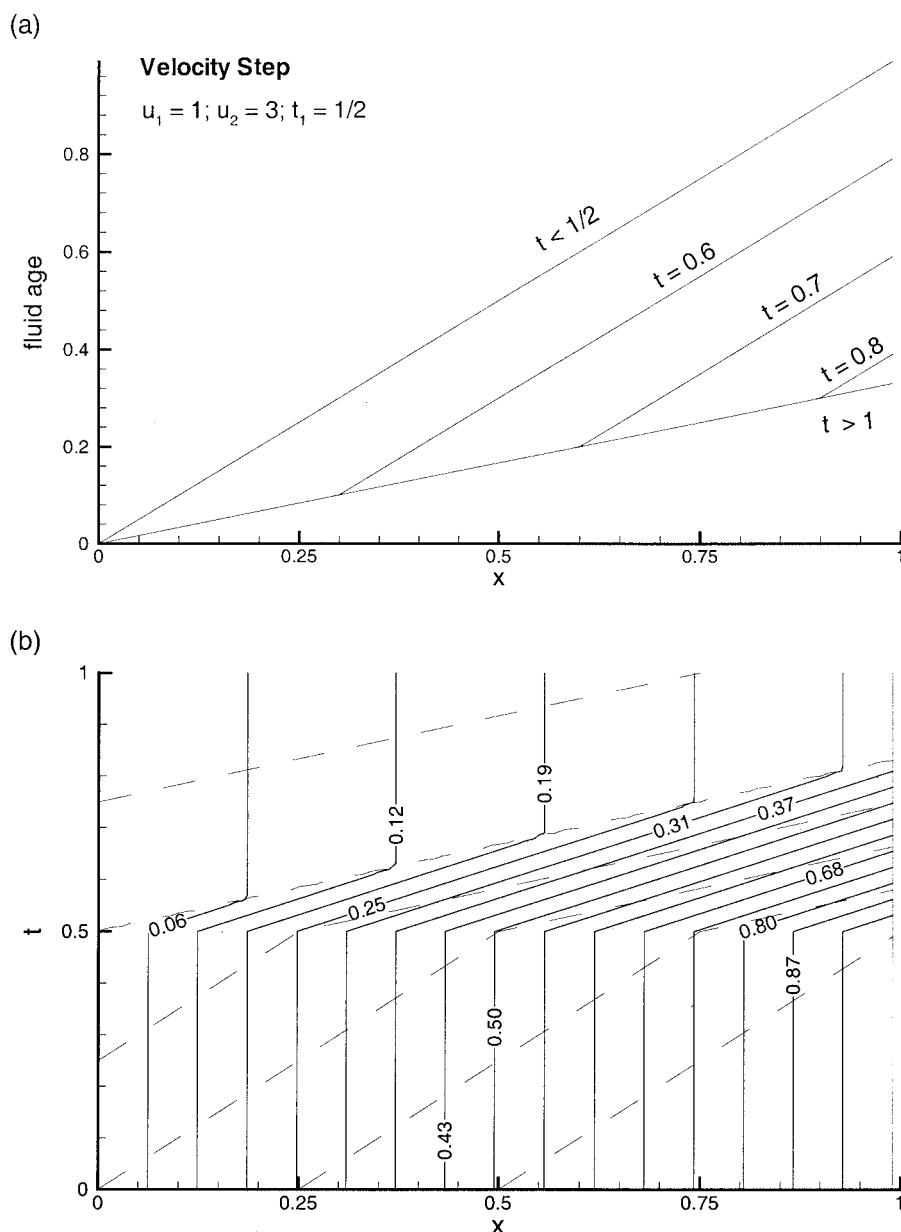


Figure 7. Evolution of the age during a velocity step.

The velocity transition from $u = 1$ to $u = 3$ occurs at time $t = 1/2$. (a) Age profile at different instant. (b) Contours of age in the (x, t) plane.

comparison between the age distribution as computed by Eq. 16 and the age obtained following fluid particles along their path will provide a real and challenging illustration of the method. The transport Eq. 16 has been numerically integrated using the imposed time-varying velocity field (Eq. 36) and using a standard first-order (upwind) finite-volume advection scheme and first-order Euler explicit time-marching scheme. The grid used consists of a 200×100 uniform Cartesian mesh, and constant time-step sizes of $\Delta t = 0.1$ were used from $t = 0$ to $t = 30$.

The results are given in Figure 9, where several lines of constant age are shown at time $t = 30$ (solid lines). As expected, age increases downstream, with the contour of age $a = 10$, for instance, representing the locus of material elements

that have entered the system at time $t = 30 - 10 = 20$. These lines of constant age should therefore be compared with the position of particles injected in the domain ($x = 0$) along various y -values, and at different earlier times $t - a$ in the past. These points are represented by the circles in the figure, and show excellent agreement, even over relatively long times (large values of age). This result gives a good illustration of the extension of the age evolution equation to unsteady flow systems. It also shows the potential of the method for obtaining valuable insights in the flow behavior of complex unsteady systems at a very low cost, given that it requires only the solution of an additional scalar transport equation. The other option would be to continue to inject a high density of discrete tracer particles into the unsteady flow and track their individual

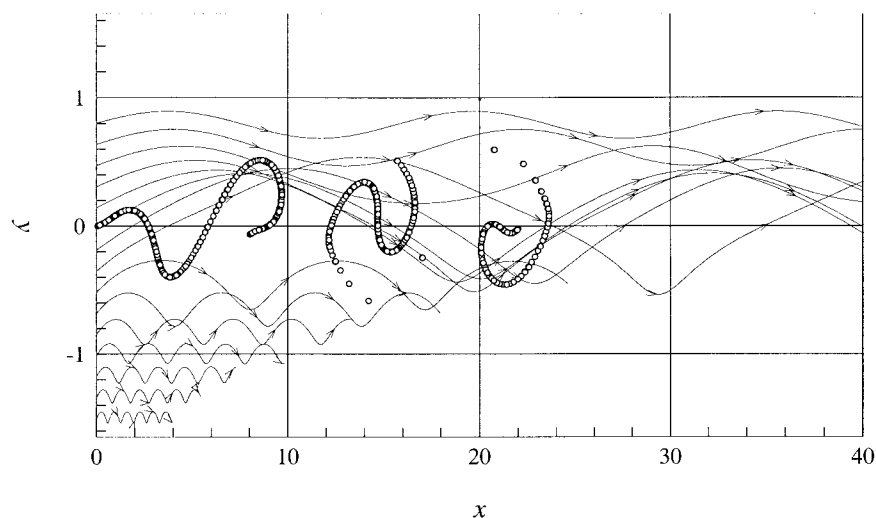


Figure 8. Streaklines (○) and streamlines (—) at time $t = 30$ for the unsteady shear flow described by Eq. 36.

positions, which would require a much higher level of computational resources, in addition to a significant programming effort.

Simple closed-flow systems

The case of a closed flow has already been encountered in a previous example with the recirculation zone in the cavity. As was pointed out, the age should increase indefinitely in such a closed system, given that fluid particles neither enter nor leave the system. This situation is intrinsically transient, with the age increasing at the same rate as the elapsed simulation time. There is, however, a value in providing a bounded version of the age in such flow configurations. In line with the definition of age used in this work, the age along closed particle paths will remain bounded by defining a region on the path where the age is reset to zero (or another finite value). In this case, the age will remain bounded and independent of time if the underlying flow field is steady. Its value at a point represents the time

taken by a fluid element to reach this point because it has left the domain where its value was defined to be zero (called the “reset” domain). This extension to a closed-flow system has obvious benefits for the study of closed flows and mixing processes, such as batch vessels and mixers, by providing better insight into fundamental mixing mechanisms and times.

These concepts can first be illustrated and validated using a simple closed-flow system. It consists of an annular domain $r_1 \leq r \leq r_2$ and $0 \leq \theta \leq 2\pi$ in which a unidirectional, steady-velocity field is defined (in cylindrical coordinates) such that $u_\theta = u_\theta(r)$ and $u_r = 0$. With this velocity field, the age evolution Eq. 16 simplifies to

$$\frac{\partial a}{\partial t} + \frac{u_\theta}{r} \frac{\partial a}{\partial \theta} = 1 \quad (37)$$

In principle, on such an annular domain the only boundary conditions that can be imposed are on boundaries $r = r_1$ and

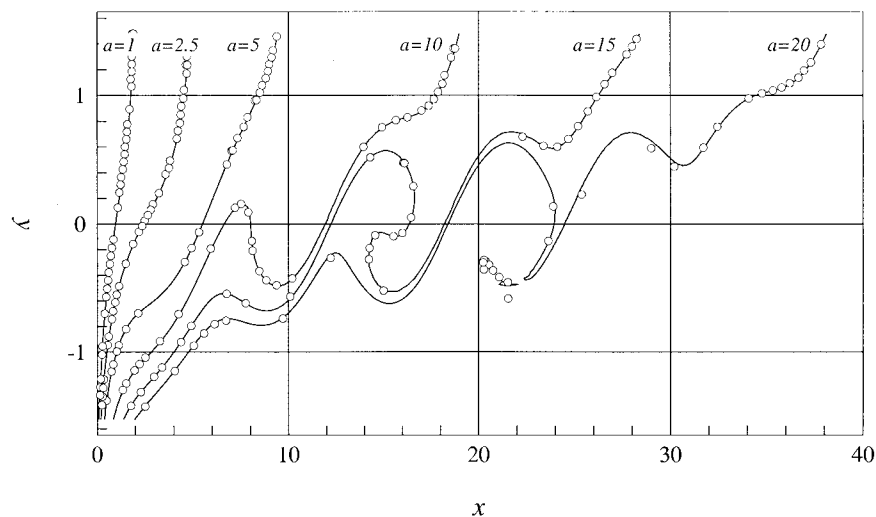


Figure 9. Comparison between the age contours computed with the evolution Eq. 22 (—) and the position of particles injected at different moments in the flow, as labeled (○).

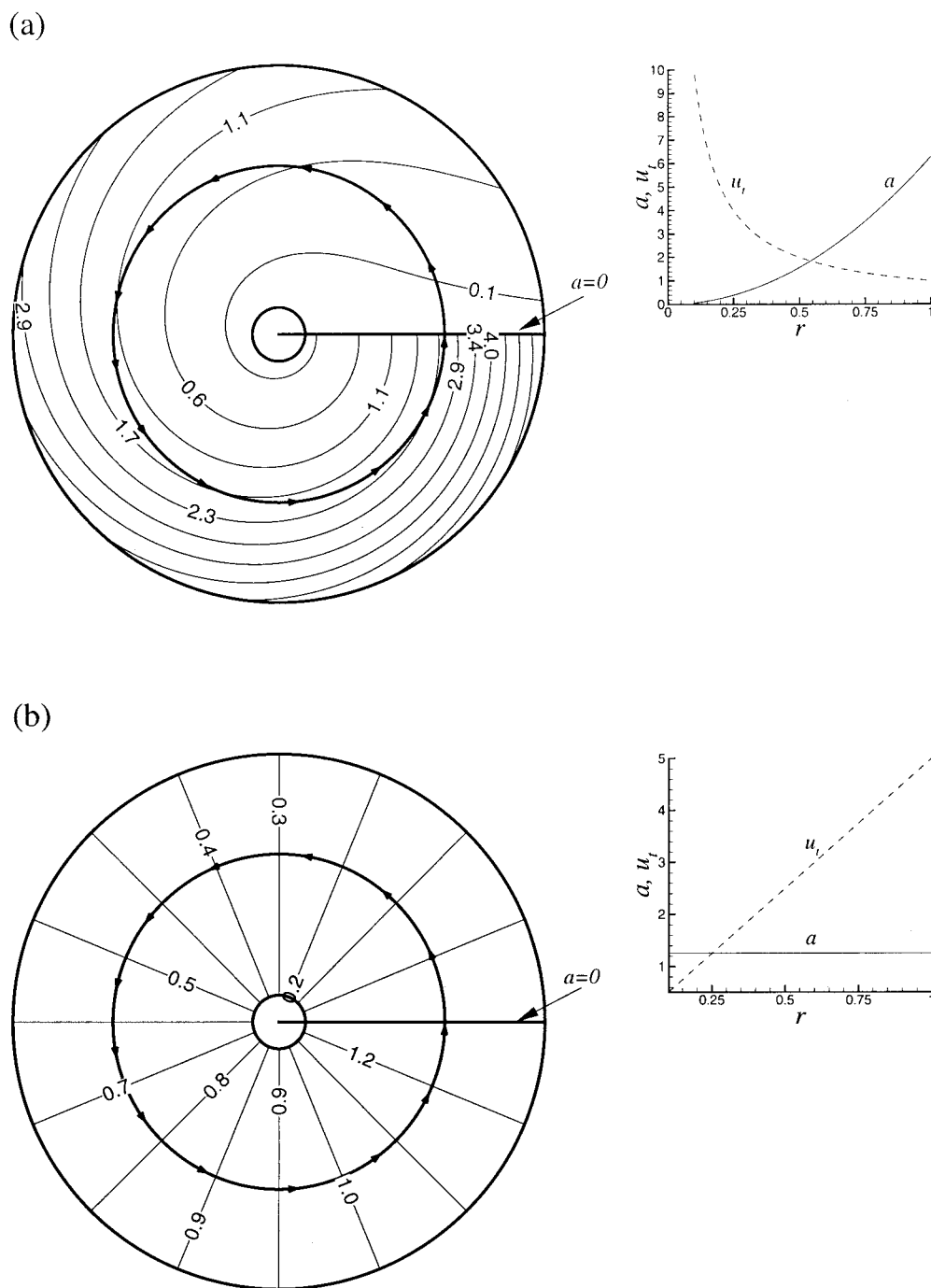


Figure 10. Contours of age in the case of a closed-flow system with age reset to $a = 0$ along the cut $\theta = 0$.

(a) Case of an irrotational velocity distribution $u_\theta = 1/r$. (b) Case of a velocity distribution $u_\theta = 5r$. In both cases, the inserts show the radial evolution of the velocity and age profiles at position $\theta = 2\pi$.

$r = r_2$. With axisymmetric boundary and initial conditions, the solution of Eq. 37 is

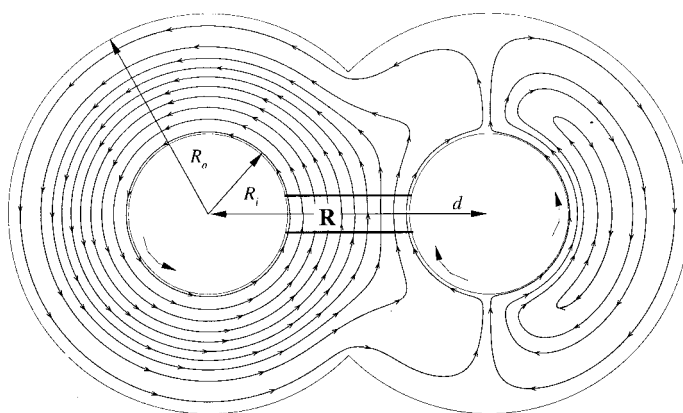
$$\frac{\partial a}{\partial t} = 1 \quad (38)$$

or $a = t$. As explained earlier, this shows that the age is an unsteady and unbounded quantity on closed streamlines, is

homogeneous in space, and is a measure of the time elapsed since the start of the flow (the start of the simulation).

Consider now the alternative situation where a cut is made in the annular domain at $\theta = 0$. In this case, it is possible to introduce the additional boundary condition $a = 0$ at $\theta = 0$, and the asymptotic solution of Eq. 37 now becomes steady and bounded, and is given by

(a)



(b)

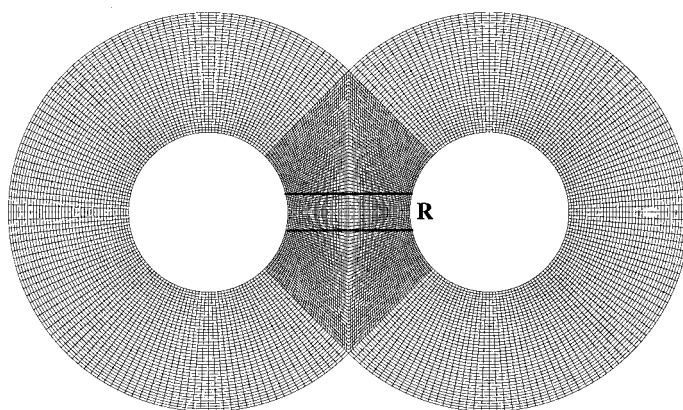


Figure 11. (a) Geometry and streamlines corresponding to the 2-D, closed-flow system; (b) computational mesh used for the numerical solution of the flow and age equations.

$$\frac{u_\theta}{r} \frac{\partial a}{\partial \theta} = 1 \quad (39)$$

or

$$a(r, \theta) = \frac{r\theta}{u_\theta} \quad (40)$$

Note that the age is no longer axisymmetric, and now depends on the spatial coordinates r and θ , contrarily to the velocity field which depends on r only. This is attributed to the fact that the cut introduced at $\theta = 0$ affects only the age evolution equation.

Obviously, formulation of the partial differential equations does not allow the imposition of such conditions outside real domain boundaries, and a cut in the domain is rather difficult to implement in an existing numerical method, especially without affecting the solution process for the fluid equations. The approach developed in the previous section gives a very simple way to implement such a cut using a suitable source term. For this, it is sufficient to define the “reset” domain \mathbf{R} in Eq. 16 or Eq. 22

$$\mathbf{R} = \{(r, \theta = 0), r_1 \leq r \leq r_2\} \quad (41)$$

This is illustrated in Figure 10, where two different profiles of the tangential velocity u_θ are used. In the first case (Figure 10a), an irrotational flow profile $u_\theta = 1/r$ is used, which gives from Eq. 40 the age distribution $a = r^2\theta$. The second case (Figure 10b) corresponds to a solid-body rotation motion defined by $u_\theta = 5r$, which gives $a = \theta/5r$.

Closed-flow systems

The previous illustration on a simple closed-flow system has shown the possibility and interest of modifying the governing age equation, but it has also highlighted the need to enforce a specific value of the age within the domain through the use of the “reset” domain \mathbf{R} . To illustrate how this would apply in a more realistic situation, an arbitrarily complex, steady, and closed-flow system has been designed, as shown in Figure 11. It consists of two overlapping annular regions ($R_o/d = 2/7$ and $R_o/d = 5/7$) with a tangential velocity imposed on the internal boundaries [$u_\theta(\theta) = 1$ on the left, and $u_\theta(\theta) = \pm 0.2$ on the right side; see Figure 11a). The region \mathbf{R} , defining the area where the age is set to zero, is shown in the figure as $\mathbf{R} = \{(x, y) \text{ s.t. } -1 \leq$

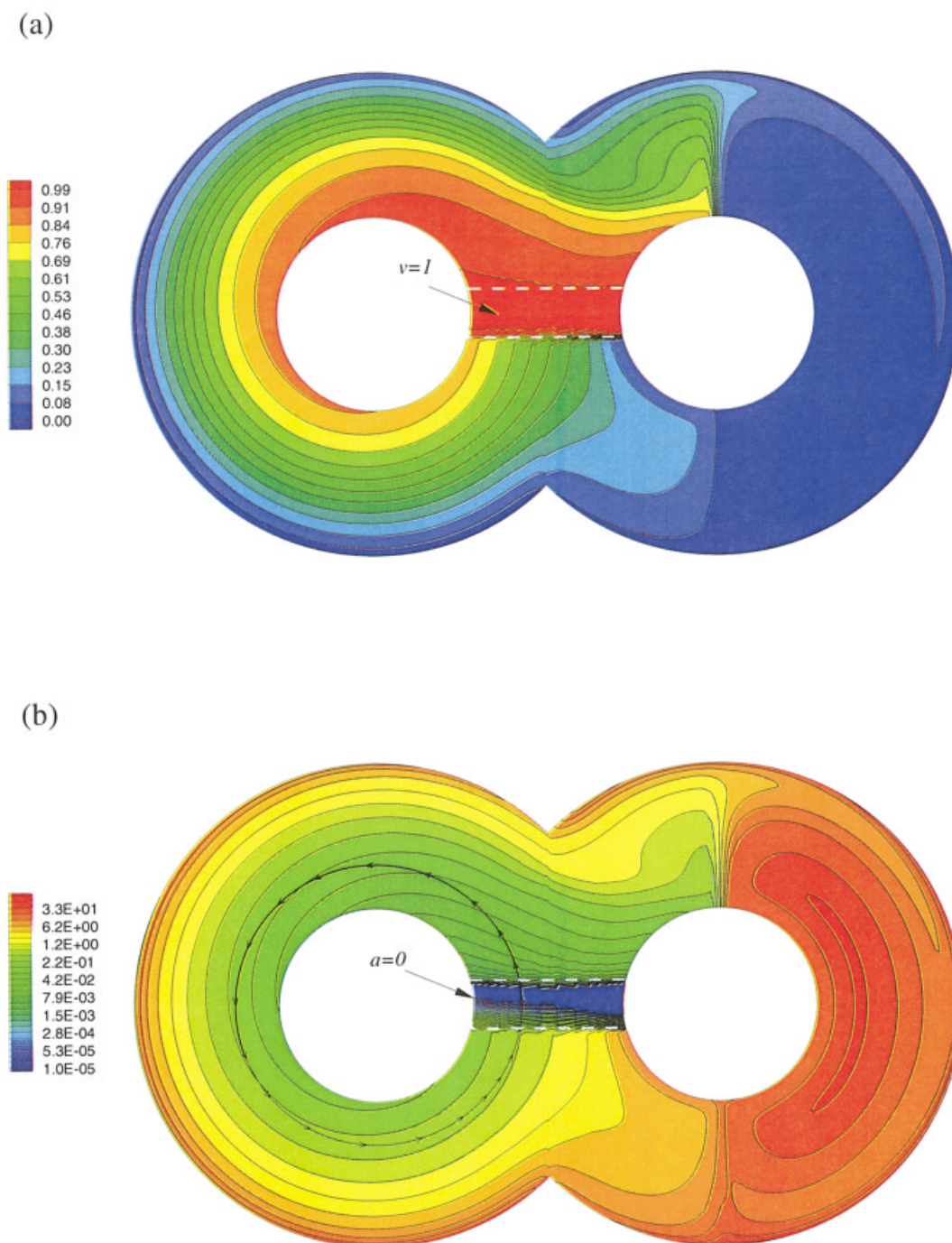


Figure 12. (a) Contour lines of the ventilation rate v ; (b) contour lines of the age a (note the logarithmic scale on the legend).

$x \leq 1$ and $-0.1 \leq y \leq 0.1$ }. The parameters entering in the age Eq. 22 are defined as $\alpha = \beta = 1$, $f_R = 1$ in the region **R** and zero otherwise, and the stiffness factor c is taken as $c = 100$. As was the case for the steady open-flow system, the flow equations have been solved to steady state using the commercial CFD software (CFX-5.1 User Manual, 2003) on an unstructured finite-volume mesh shown in Figure 11b. This relatively coarse mesh has over 8000 nodes, and a standard first-order discretization has been used. Equation 22 has been

solved based on the flow field obtained by first solving the steady flow equations.

Figure 12a shows contours of the ventilation rate v , and Figure 12b gives the corresponding age contours. As expected, the age remains bounded to low values in the domain where streamlines cross the region **R**. On the other hand, the age should continue to increase in the other closed-flow region on the right-hand side of the system because those streamlines do not cross the “reset” region **R**. However, some leakage through

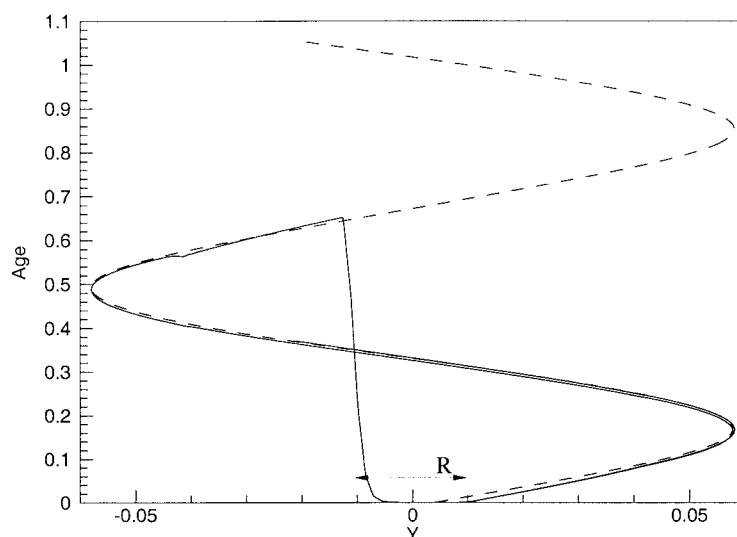


Figure 13. Evolution of the age along the streamline shown in Figure 11b.

Age computed from the evolution Eq. 22 (—); age computed from its Lagrangian definition (---).

numerical diffusion is visible and will effectively put an upper bound on the values of the age by limiting the size of the gradient across the two closed-flow regions. Obviously, a more accurate numerical scheme would lower the numerical diffusion and could permit a better assessment of the precise effect of the diffusion on the solution. Concerning the behavior of the solution over the “reset” domain, the age has a rapid decrease within the thickness of **R**, as is visible in Figure 12b where high gradients of age exist as the fluid enters the region **R**. This suggests that the value of the stiffness parameter c has been appropriately chosen.

As before, it is useful to compare the results obtained by solving the age evolution equation to the Lagrangian age computed by integrating the residence time along a particle path. This is done in Figure 13 using the streamline shown in Figure 12b. The figure shows the evolution of the age along the y -coordinate, with the solid line corresponding to the age obtained from its evolution (Eq. 22). The agreement with the “real” Lagrangian age (dashed line) is remarkable. The sharp exponential decrease of the age over the **R** region (corresponding to values $-0.1 \leq y \leq 0.1$) is also visible.

Conclusions

The age-of-fluid method has been revisited to evaluate and extend it from its traditional application domain of steady, open-flow systems to general unsteady and/or closed-flow systems.

The most significant change in the approach has come from the definition of the age of the fluid in a purely kinematic way as a tagging variable, and based solely on the velocity field of the underlying fluid. All the other methods proposed in a Eulerian context somehow determine the age indirectly by tracking an injected tracer material in the flow domain.

The resulting mathematical formulation is formally very similar to the classical age-of-fluid transport equations previously obtained, but with the benefit of clarifying a number of issues such as the effect of the value of the diffusion coefficient, the definition of suitable boundary conditions, the vali-

dation in the case of unsteady-flow conditions, and the extension to closed-flow domains by using an appropriate modification of the source term in the age transport equation.

More than a purely numerical revisiting of previous work, it has been shown that the proposed formulation can provide novel and relevant insight into the transport and mixing phenomena in unsteady and closed flows that are otherwise difficult to study. For unsteady flows, using the appropriate definition of the fluid age, it gives a very rich view into some essential mixing parameters at a very low (computational) cost because it requires the solution of only one additional scalar transport equation. In the same way, closed-flow systems, which are by definition difficult to probe or analyze by injection of a tracer, could now be studied with a new tool with which the advective age distribution from a given internal “injection” point would show a characteristic pattern related to some essential mixing mechanism.

In addition, an original and challenging validation method has been used, which compares the age obtained in the Eulerian computational framework to the “real” Lagrangian age evolution along particle paths.

Finally, very large values (theoretically infinite) encountered in the numerical treatment of the age evolution equation have been appropriately dealt with by using a suitable transformation of variables, together with the appropriate change in boundary conditions.

Literature Cited

- Baléo, J.-N., and P. Le Cloirec, “Validating a Prediction Method of Mean Residence Time Spatial Distributions,” *AIChE J.*, **46**, 675 (2000).
- Beckers, J. M., E. J. M. Delhez, and E. Deleersnijder, “Some Properties of Generalized Age-Distribution Equations in Fluid Dynamics,” *SIAM J. Appl. Math.*, **61**, 1526 (2001).
- CFX-5.1 User Manual, AEA Technology, Harwell, UK.
- Danckwerts, P. V., “Continuous Flow Systems: Distribution of Residence Times,” *Chem. Eng. Sci.*, **2**, 1 (1953).
- Danckwerts, P. V., “Local Residence Times in Continuous Flow Systems,” *Chem. Eng. Sci.*, **9**, 78 (1959).
- Davidson, L., and E. Olsson, “Calculation of Age and Local Purging Flow Rate in Rooms,” *Bldg. & Environ.*, **28**, 12 (1987).

- Deleersnijder, E., J. M. Campin, and E. J. M. Delhez, "The Concept of Age in Marine Modelling. I. Theory and Preliminary Model Results," *J. Marine Syst.*, **28**, 229 (2001).
- Delhez, E. J. M., J. M. Campin, A. C. Hirst, and E. Deleersnijder, "Toward a General Theory of the Age in Ocean Modelling," *Ocean Modell.*, **1**, 17 (1999).
- Hama, F. R., "Streaklines in a Perturbed Shear Flow," *Phys. Fluids*, **5**(6), 644 (1962).
- Hunter, J. R., P. D. Craig, and H. E. Phillips, "On the Use of Random Walk Models with Spatially Variable Diffusivity," *J. Comp. Phys.*, **106**, 366 (1993).
- Levenspiel, O., "The Coming-of-Age of Chemical Reaction Engineering," *Chem. Eng. Sci.*, **35**, 1821 (1980).
- Levenspiel, O., *Chemical Reaction Engineering*, 3rd Edition, Wiley, New York (1999).
- Nauman, B. E., "Residence Time Distributions and Micromixing," *Chem. Eng. Commun.*, **8**, 53 (1981).
- Patankar, S. V., *Numerical Heat Transfer and Fluid Flow*, Hemisphere Publishing, Washington, DC (1980).
- Sandberg, M., "What is Ventilation Efficiency?" *Bldg. & Environ.*, **16**(2), 123 (1981).
- Sandberg, M., and M. Sjöberg, "The Use of Moments for Assessing Air Quality in Ventilated Rooms," *Bldg. & Environ.*, **18**(4), 181 (1983).
- Spalding, D. B., "A Note on Mean Residence Times in Steady Flows of Arbitrary Complexity," *Chem. Eng. Sci.*, **9**, 74 (1958).
- Weinstein, H., and M. P. Dudukovic, "Tracer Methods in the Circulation," *Topics in Transport Phenomena*, C. Gutfinger, ed., Wiley, New York, pp. 345–356 (1975).
- Wen, C. Y., and L. T. Fan, *Models for Flow Systems and Chemical Reactors*, Marcel Dekker, New York (1975).
- Zwietering, T. N., "The Degree of Mixing in Continuous Flow Systems," *Chem. Eng. Sci.*, **11**, 1 (1959).

Manuscript received Jul. 24, 2003, and revision received Dec. 8, 2003.